BioGecko

Vol 12 Issue 01 2023
ISSN NO: 2230-5807

MICROSCOPIC ANALYSIS AND DURABILITY STUDIES ON HIGH AND LOW CALCIUM FLYASH BASED GEO POLYMER CONCRETES DEVELOPED WITH ALTERNATIVE CONCRETING INGREDIENTS

S. Jagadeesan [1*] and Dr. M. Purushothaman [2]

[1], Research Scholar, Department of Civil & Structural Engineering, Annamalai University, Annamalainagar-608002, Tamilnadu, India, Email: jagadeesanaee1@gmail.com

[2], Associate Professor, Department of Civil & Structural Engineering, Annamalai University, Annamalainagar-608002, Tamilnadu, India, Email: emp4624@gmail.com

***Corresponding Author**

Abstract

Concrete as a construction material proved to be an inevitable in construction industry for its strength and flexibility of its desired shape. At the same time, the concern for enduring nature is still lagging due to its nexus with the drastic environmental exposure hazards. Despite the fact concrete being stronger, the influx of environmental severity plays a misery action in the aging of concrete. Studies on the long-term durability of concrete has provided controlling measures from further deterioration. However, the prevention of concrete from the perils of hazardous environmental exposures and erratic climatic conditions persists for intense research investigations. From previous researches and literatures, it was found that Geo Polymer Concrete (GPC) made from industrial by-product wastes proved to be a viable and economical solution for this bottleneck issue. In this study, the efficacy of geopolymer concrete made from both class-C and class-F flyash and replacing the conventional fine aggregate and coarse aggregate with M-sand and steel slag respectively was experimentally investigated for durability and microstructural properties. The outcome of the test results demonstrated a convincing performance of geopolymer concrete in comparison with the conventional concrete, which is made from the deep extraction of natural resources.

Keywords: climate, deterioration, durability, damage, environment, endure, exposure, hazards, long-term, microstructure

1 Introduction

The robust manufacturing of cement in manufacturing industries and enormous consumption of concrete material in construction industries has led to the apprehensions of the environmental fraternity due to the startling discharge of carbon footprints on the planet. The risk posed in front of the scientific community has successfully emerged with a turnaround solution of evolving potential construction materials from the discarded industrial waste by-products. The formidable task of bridging the gap between waste disposals to recycle/reuse material by the innovators has resulted in multifold benefits for the construction sectors.

The alternative materials replacing the conventional materials for concrete making has achieved desired outcomes. Various alternative binding materials like Flyash, Rice Hush Ash, GGBS, Metakaolin, Silicafume, etc replace the binder material cement in conventional concrete. In case of conventional fine aggregate, natural river sand is replaced by M.sand, Granite powder, Ceramic powder, Quarry dust, etc. Similarly, the conventional coarse aggregate crushed stone gravel is replaced by steel slag, copper slag,

flyash slag, etc. These alternative materials shall be synthesized in appropriate mix proportions and ratios with the help of alkali solutions to form a green concrete or ecofriendly concrete called geopolymer concrete. The geopolymer concrete shall be tailor-made to suit our strength requirements. Earlier researches and literatures has found geopolymer performing excellent when it comes to durability requirements apart from its strength capacities.

The microstructure of geopolymer paste and mortar derived from class-C fly ash was studied using XRD.The microstructure of geopolymer paste and mortar derived from class-C fly ash was studied using XRD.revealed the unreacted quartz, some reacted components and gel formation in the samples whereas the SEM analysis shown that reacted product made a coverage around the unreacted particles and the dense structure contributed to the higher compressive strength, Xueying Li et. al., (2013). The replacement of M.sand for natural river sand in producing flyash based geopolymer concrete proved to be an excellent resistance material against acid and sulphate attacks due the formation of stronger polymer chain during the poly condensation reaction, K. Arul Priya (2016). The thermal endurance of flyash based geopolymer concrete (GPC) made with M.sand as fine aggregate when subjected to higher temperatures up to 800ºC proved to be substantial when compared to ordinary Portland cement concrete (OPC) that sustained compressive strengths at elevated temperatures ranging from 200ºC to a maximum of 400ºC. Meanwhile the thermal insulation capacity of GPC was equivalent to OPC whereas the heat dissipating capacity of GPC was higher than OPC, Chithambar Ganesh. A (2018). The loss of weights and compressive strength of GPC (flyash based made with M.sand as fine aggregate) and OPC was a result of increase in temperature from 200ºC to 600ºC as well as its corresponding increase in duration from 1 to 6 hours. In addition, the increase in grades of concretes resulted in deficit strength at the helm of its brittleness and dense microstructure. However, as a measure of thermal resistance, the strength losses experienced by GPC was comparatively lower than OPC at elevated temperatures, T. Srinivas and P. Geethanjali Rathod (2018). In the case of flyash based geopolymer made with steel slag as coarse aggregate, the compressive strength of geopolymer concrete increased due to decrease in water absorption and apparent volume of permeable voids when compared to conventional concrete, O. M. Omar et. al., (2015). Similarly, the durability report of flyash based geopolymer concrete made with partial replacements of steel slag as coarse aggregate when exposed to severe environments showed an excellent resistance against acid and sulphate attacks with a trailing in strength caused by the porosity of slag aggregates, Suganya. N and Thirugnanasambandam. S (2019).

Researchers in this study looked at the durability and microstructure characteristics of geopolymer concrete made with flyash binders of class C or Class F and with different types of aggregates. The durability requirements pertaining to water absorption, acid and sulphate attacks and thermal resistance at elevated temperatures was performed. Moreover, the morphology and chemical composition of the geopolymer concrete specimens were analyzed through SEM and XRD respectively.

2. MATERIALS AND METHODS

2.1 Binder Materials

Cement and flyash from thermal power plants in Tuticorin, Mettur, and Neyveli were used as binders in the concrete mixture, according to IS 8112-2013. Depending on the calcium content, flyash from thermal power plants was categorised into class-C and class-F flyash, respectively.

The physical properties of binder materials are given in Table 1a.

Table 1a. Physical Properties of Binder Materials

Property	Cement	Flyash	
	OPC 43 Grade	Class C – High Calcium	Class F – Low Calcium
Specific Gravity	3.15	1.92	2.12
Fineness (m2/kg)	225	372	376
Initial Setting Time (min.)	30	35	37
Final Setting Time (min.)	600	548	554

The chemical composition of binder materials are given in Table 1b.

Table 1b. Chemical Composition of Binder Materials

Cement - - OPC 43Grade		Flyash-Class C		Flyash-Class F	
Elements	% Mass of Elements	Elements	% Mass of Elements	Elements	% Mass of Elements
SiO_2	22.65	SiO_2	35.7	SiO_2	38.6
Al_2O_3	04.32	Al_2O_3	15.8	Al_2O_3	16.5
Fe_2O_3	02.33	$Fe2O_3$	16.1	Fe_2O_3	17.1
CaO	64.32	CaO	34.85	CaO	15.6
Na_2O	00.06	TiO_2	0.46	TiO_2	1.35
K_2O	00.05	K_2O	1.85	K_2O	2.18
TiO_2	-	MnO	0.16	MnO	0.15
MgO	02.23	Na_2O	0.19	SO_3	3.05
SO_3	02.12	P_2O_5	0.04	NiO	0.05
LOI	02.12	LOI	1.11	CuO	0.08

Table 1b presents the dissemination of the key elements present in different classes of fly ash determined from X-Ray Fluorescence (XRF) analysis. The total amount of silicon, aluminium and ferrous oxides of class-C and class-F flyash was 67.6 % and 72.2 % respectively while the composition of calcium oxides of class-C and class-F flyash was 34.85% and 15.6% respectively. The mass ratio of SiO_2 to Al_2O_3 determines the synthesis and application of geopolymer materials and from the XRF analysis, it was found as 2.26 for class-C flyash and 2.33 for class-F flyash. From previous researches, it was found that geopolymer prepared with ASTM class-F fly ash was preferable compared to ASTM Class-C due to flash setting of class-C flyash.

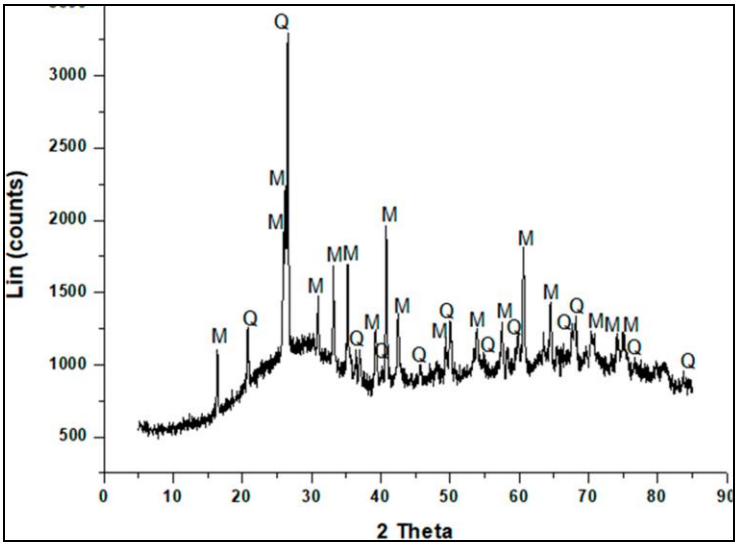

Fig. 1 Qualitative XRD of Flyash [Q = Quartz, M = Mullite]

X-Ray Energy dispersive (XRD) analysis of a fly ash sample yielded the mineral phases depicted in Figure 1. Crystal (SiO2) and Mullite (3Al2O32SiO2) were found in flyash, with low intensity diffraction peaks showing the presence of these two major phases. Flyash's amorphous glassy phase showed up as a broad band in the XRD spectrum, spanning 20° to 40° in 2. Biosensor and X - ray fluorescence analysis revealed that quartz and mullite had higher percentages of silica and alumina than the other samples studied. The results of the XRF and XRD tests were found to be in agreement. A geopolymer product can be formed from flyash at mild temperatures, whereas quartz and mullite must be fused at high temperatures to release their silica and aluminium content.

As can be seen in Figures 2A & 2B, different magnifications of the same fly ash sample were used to obtain SEM images. The flyash particles were spherical in shape and some of the particles being closely attached, results in agglomerates. It happens because of thermo chemical transformation of mineral particles occurring during the coal combustion process followed by rapid cooling which tends the minerals to produce small droplets/grains in the form of spherical shape. Moreover, the outer smooth surface of the flyash particles was achieved by presence of aluminosilicate glassy phases.

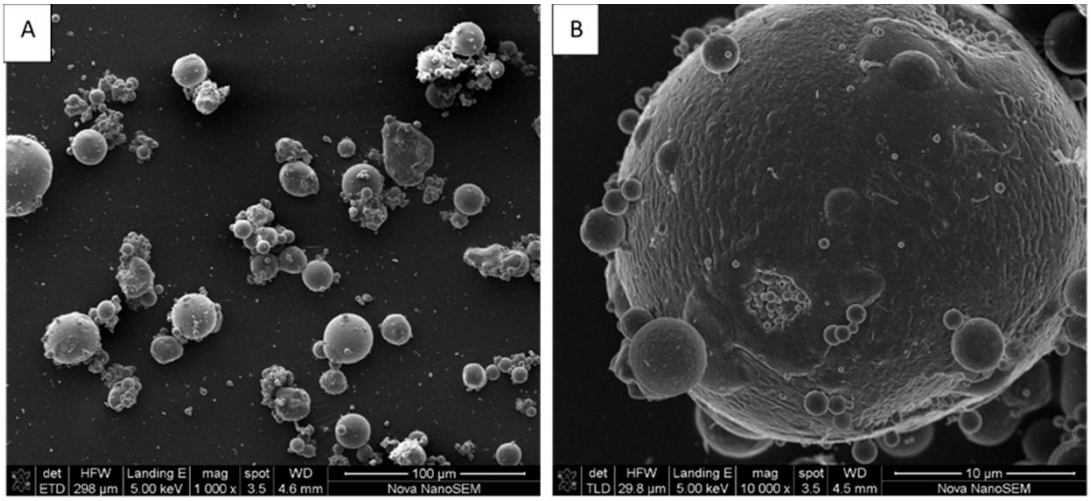

Figure 2. SEM Micrographs of Flyash Particle Sizes at Magnifications (A) 1000×, and (B) 10,000×

2.2 Fine Aggregate

PCC was made from fine aggregates ranging in size from 75 m to 5 mm, which were derived from locally available natural river sand and met the requirements of IS 383-1970. Crushed hard stone aggregates were used to make M.sand, which was then used to make GPC. Natural sand was purchased from local stone quarry suppliers. Organic impurities were absent from the manufactured sand, which meets the requirements of IS 383 – 1970. Table 2 lists the results of tests on the required fine aggregate properties.

Table 2. Properties of Fine Aggregate Materials

Properties	**River Sand**	**M. Sand**
Specific gravity	2.67	2.66
Fineness modulus	3.15	4.28
Bulk density (kg/m3)	1667	1751
Water absorption (%)	1.0	0.92
Grading Zone	Zone – II	Zone – II
Size	Passing through 4.75 mm sieve	Passing through 4.75 mm sieve

2.3 Coarse Aggregate

PCC coarse aggregates were crushed angular stone aggregates of maximum size 20mm in accordance with IS 383-1970. Steel slag was used as the coarse aggregate in GPC. The impurities and fluxing agents that form the liquid slag floating above the liquid crude iron or steel in electrical arc furnaces collected from the hot-rolling steel mill in Madagadipet, Pondicherry, India, formed this byproduct during the melting of steel scrap. Air dried large boulders of slag were used for laboratory

testing, and then crushed and sieved with an IS 4.75mm sieve to a size similar to natural coarse aggregate. Laboratory tests have yielded the physical and mechanical properties of bristly aggregate materials.

Table 3a. Physical and Mechanical Properties of Coarse Aggregate Materials

Properties	Crushed Stone / Gravel	Steel Slag
Specific Weight	2.63	3.2
Fineness Modulus	6.32	2.86
Bulk Density (kg/m3)	1336	1040
Water Absorption (%)	0.50	2.86
Moisture Content (%)	0	0.25
Maximum Size (mm)	20	20 below
Crushing Coefficient (%)	25	12.4
Abrasion Index (%)	34	14.5
Impact Resistance (%)	32	15.0

The chemical analyses test report of the local steel slag used as an alternative coarse aggregate material for conventional coarse aggregate (crushed stone aggregate) obtained from the manufacturer is given in Table 3b. In situations where slag aggregates are used, IS 456-2000 validates that slag aggregates should not contain more than 0.5% of sulphates in the form of SO_3 and 10% of water absorption.

Table 3b. Chemical Analysis of Local Steel Slag Aggregates

Constituent	Composition %
SiO_2	13.15
Fe_xO_y	36.78
Al_2O_3	5.57
CaO	33.05
MgO	5.029
MnO	4.162
Cr_2O_3	0.786
P_2O_5	0.753
TiO_2	0.596
V_2O_5	0.106
SO_3	0.145

2.4 Mixing Agents

IS 456-2000 suggests that water used for mixing and curing shall be clean and free from deleterious substances that may be hazardous to concrete or steel. Hence, potable water of pH 6.5 was used for the preparation of PCC. For producing GPC, Alkaline Activator Solution (AAS) was used as a

mixing agent for binder and aggregate materials. AAS was obtained from the concentrations of sodium hydroxide (NaOH) pellets and sodium silicate (Na2SiO3) liquid. The molar concentration of sodium hydroxide attempted in this study was 8M and 14M. It contained 37.6 percent solids, 28.7 percent silicate, and 8.9 percent sodium, making up 62.4 percent of the total solution. Calculating the molar mass of NaOH, which contains 22.99 g/mol of Na, 16.00 g/mol of O, and 1.008 g/mol of H, yielded a sodium hydroxide preparation for one litre of distilled water. 1M of NaOH is equal to 40g of NaOH granules because the total molar mass is 40g.To reduce water content and to achieve desired workability of more than 100mm slump, superplasticizer-CONPLAST 430 was used.

2.5 Design Mix Proportions and Quantities

The durability of concrete was tested for a cube compressive strength of 30 MPa and the design mixes for conventional concrete M30 grade and geopolymer concrete G30 were made accordingly. The mix proportions and quantities of PCC-M30 are given in Table 4a.

Table 4a. Mix Proportions and Quantities of PCC

Material	**Binder: Cement**	**FA: R. Sand**	**CA: Gravel Stone**	**Water**	**Superplasticizer**
Quantity (kg/m3)	426	598	1266	192	Nil
Proportion	1	1.40	2.97	-	-
Note: W/c ratio = 0.45					

The mix proportions and quantities of GPC-G30 are given in Table 4b.

Table 4b. Mix Proportions and Quantities of GPC

Material	**Binder: Flyash**	**FA: M. Sand**	**CA: Steel Slag**	**Sodium Silicate Solution (Na2SiO3)**	**Sodium Hydroxide Solution (NaOH)**	**Extra Water**	**Super plasticizer**
Quantity (kg/m3)	408	554	1294	103	41	14.5	10.2
Proportion	1	1.36	3.17	0.25	0.10	-	-
Note: 1. Binder: Class-C and Class-F flyash 2. Curing: Ambient curing (room temperature of 30ºC) for class-C flyash GPC and Heat curing (60ºC for 24 hrs in oven) for class-F flyash GPC 3. Molar concentration of NaOH = 8M and 14M 4. Alkali Activator Solution (AAS) ratio = Na2SiO3 / NaOH = 2.0 5. Liquid / Binder ratio = AAS / Flyash = 0.35 6. Extra water added to the mix for moisture requirement = 3.5% Wt. of Binder 7. Superplasticizer added to the mix on workability criteria = 2.5% Wt. of Binder							

Figure 3 shows the typical SEM image of a flyash based geopolymer concrete mix.

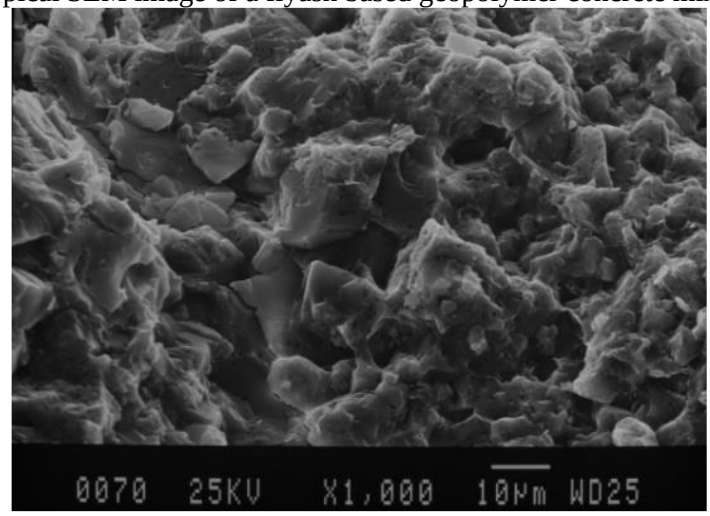

Figure 3. SEM Analysis of Concrete Mix

3. EXPERIMENTAL TESTS

Class-F low calcium and class-C high calcium flyash-based GPC were compared to PCC in order to study the durability behaviour, and differential curing conditions were applied to the cube concrete specimens.. The percentage loss of weight and residual compressive strength of concrete specimens after immersion in differential curing conditions determines the durability criterion. The cube concrete specimens immersed in water, acid and sulphate solutions are shown in Figure 4.

a. Water

b. Acid Solution

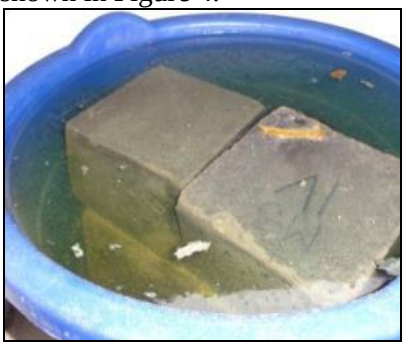

c. Sulphate Solution

Figure 4 Differential Curing Conditions to Determine Residual Compressive Strength of Concrete Specimens

3.1 Water Absorption Test

After 28 days of curing, the PCC and GPC specimens were subjected to a water absorption test in accordance with ASTM D570-98. The volume of water soaked up by the corresponding concrete samples was determined by conducting this test. At a temperature of approximately 23oC for 24 hours, 7, 14, and 28 days, the concrete samples were weighed oven dry before being placed in a bucket of water. Afterwards, the wet samples are collected out, patted, dried, and weighted. As a result, the bulk density was expressed as a percentage of body weight.

3.2 Acid Attack Test

The PCC and GPC samples were tested for acid resistance using 150 x 150 mm concrete cube specimens. For seven, fourteen, and 28 days, the cube specimens were weighed and immersed in water diluted with 5% Hydrochloric acid (HCl). To complete the experiment, the samples were removed from the acid solution and cleaned before being weighed and compressed. Finally, the average weight loss and compressive strength of the concrete samples were calculated.

3.3 Sulphate Attack Test

Concrete cubes of 150 x150 mm were immersed in 5 percent Magnesium Sulphate solution for 28 days, 56 days, and 90 days, respectively, for the sulphate attack test. Sulphate attack-resistant concrete mixes are put through this type of rapid testing procedure to see how well they perform. After seven, 14, and 28 days, this same weight losses and retained compressive strength of said specimens were analysed to determine how much sulphate had taken hold.

3.4 Elevated Temperature Test

Heat tests on PCC and GPC design mix samples were used to examine the effects of thermal exposure on concrete specimens. Muffle furnaces were used to study the thermal behaviour of concrete specimens exposed to temperatures ranging from 100oC to 800oC. For 1hr, 2hr, 4hr, 6hr, and 8hr, the specimens were heated in a Muffle furnace for 200oC for curing for 28 days before their initial weights were taken. The specimens were then taken out of the Muffle furnace and tested for weight loss and residual compressive strength.

3.5 Insulation Capacity Test

This is simple type of test wherein the PCC and different flyash based GPC samples were tested for its behaviour against the thermal insulation capacity by exposing it directly to the daylight sun on a hot sunny day from 9am to 6pm. The differential temperature occurring in the specimen was recorded using an Infrared thermometer at every one-hour interval. As a result, the specimen, which experienced a temperature drop, was regarded as the best insulated concrete specimen among the tested samples.

3.6 Heat Dissipation Test

An electric Muffle furnace was used to heat the PCC and GPC specimens to 300oC and then allow them to cool at room temperature. Every minute, the temperature was monitored with an infrared torch thermometer. An excellent heat dissipation property was discovered in the specimen that recovers quickly.

4. TEST RESULTS AND DISCUSSION

The specifications of concrete used in this study is demonstrated in Table 5.

Table 5. Specifications of Concrete

PCC-M30	Plain Cement Concrete of M30 grade
GPC-C8M	Geo Polymer Concrete of fck 30MPa with class-C flyash and 8 Molar concentration of NaOH
GPC-C14M	Geo Polymer Concrete of fck 30MPa with class-C flyash and 14 Molar concentration of NaOH
GPC-F8M	Geo Polymer Concrete of fck 30MPa with class-F flyash and 8 Molar concentration of NaOH
GPC-F14M	Geo Polymer Concrete of fck 30MPa with class-F flyash and 14 Molar concentration of NaOH

4.1 Differential Curing Conditions

4.1.1 Density

Table 6 shows the test results pertaining to residual weight and percentage loss of weight of concrete specimens when subjected to 28 days differential curing conditions.

Table 6. Reduction and Loss in Density of Concrete Specimens due to 28 days Differential Curing Conditions

Specimen ID	Pre-curing Weight of Specimen	Water Curing		Acid Curing		Sulphate Curing	
		Residual Weight	Loss of Weight	Residual Weight	Loss of Weight	Residual Weight	Loss of Weight
	kg	kg	%	kg	%	kg	%
PCC-M30	8.02	7.62	4.99	6.88	14.21	6.73	19.17
GPC-C8M	8.09	7.71	4.70	7.17	11.37	7.02	15.24
GPC-C14M	8.19	7.92	3.30	7.09	13.43	6.94	18.01
GPC-F8M	8.18	7.86	3.91	7.13	12.84	6.98	17.19
GPC-F14M	8.12	7.86	3.20	7.11	12.44	6.96	16.67

Figure 5 shows the variations in the residual weight and percentage loss of weight of concrete specimens when subjected to 28 days differential curing conditions.

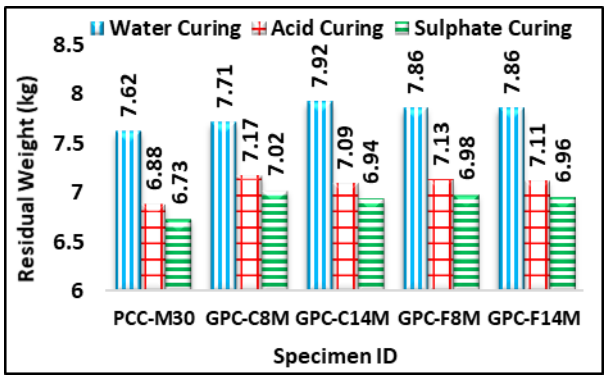

a. Residual Weight

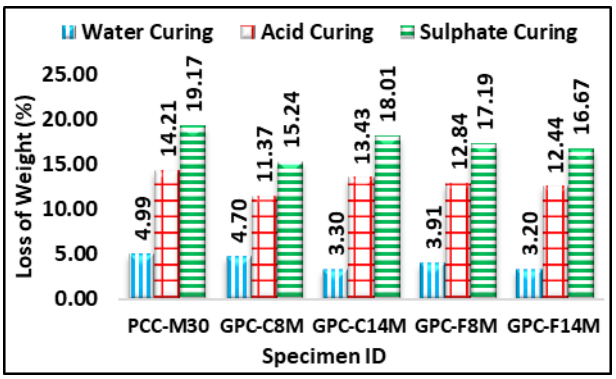

b. Loss of Weight

Figure 5. Density Variation of Concrete Specimens in Differential Curing Conditions

According to the findings (Table.6 and Figure.5), as the final geopolymer concrete mix's NaOH concentration increased from 8 M to 14 M, the water absorption decreased as well. Low water content and high alkaline formulations produced a less porous, stronger structure with lower water penetration. Low porosity, which reflects the pore size of the geopolymer material and contributes to its strength, was found to be the cause of the low water absorption. In the geopolymer mixture, large gel crystals formed with trapped water inside when a large amount of water was added. The product became more porous as the water evaporated from the pores during the 24-hour heat curing process at 60 C. This increased the amount of water absorption. Due to increased capillary porosity of concrete, concrete mixes with local steel slag as a replacement for crushed stone aggregates had low water absorption. Because geopolymer concrete had a low water absorption rate, it required only a small amount of additional water for the mixing process, whereas conventional PPC required more water because of its greater demand during mixing. Compared to natural river sand used in conventional cement concrete, M.sand as fine aggregate in flyash-based geopolymer concrete showed excellent resistance to acid attack and sulphate attack.

During the poly-condensation reaction in geopolymer concretes, a stronger polymer chain is formed. According to the findings (Table.6 and Figure.5), as the final geopolymer concrete mix's NaOH concentration increased from 8 M to 14 M, the moisture content decreased as well. Low water content and high alkaline formulations produced a less porous, stronger framework with lower water penetration. Low porosity, which reflects the pore size of the nanocomposites and contributes to its strength, was found to be the cause of the low water absorption. In the geopolymer mixture, large gel crystals formed with trapped fluid inside whenever an large amount of water was added. The product became more porous as the water evaporated from the pores during the 24-hour heat curing process at 60 C. This increased the amount of water absorption. Due to increased capillary porosity of concrete, concrete mixes with local steel slag as a replacement for crushed stone aggregates had low water absorption. Because geopolymer concrete had a low water absorption rate, it required only a small amount of additional water for the mixing process, whereas conventional PPC required more water because of its greater demand during mixing. Compared to natural river sand used in conventional cement concrete, M.sand as fine aggregate in flyash-based geopolymer concrete showed excellent resistance to acid attack and sulphate

attack. During the poly-condensation reaction in geopolymer concretes, a stronger polymer chain is formed.

4.1.2 Compressive Strength

Table 7 shows the test results pertaining to residual compressive strength and percentage loss of compressive strength of concrete specimens when subjected to 28 days differential curing conditions.

Table 7. Reduction and Loss in Compressive Strength of Concrete Specimens due to 28 days Differential Curing Conditions

Specimen ID	Water Curing	Acid Curing		Sulphate Curing	
	Compressive Strength	Residual Compr. Strength	Loss of Compr. Strength	Residual Compr. Strength	Loss of Compr. Strength
	MPa	MPa	%	MPa	%
PCC-M30	36.84	33.25	9.74	32.81	10.94
GPC-C8M	37.35	35.48	5.01	35.04	6.18
GPC-C14M	38.52	35.98	6.59	35.54	7.74
GPC-F8M	45.11	43.71	3.10	43.27	4.08
GPC-F14M	61.28	59.41	3.05	58.97	3.77

Figure 6 shows the variations in the residual compressive strength and percentage loss of compressive strength of concrete specimens when subjected to 28 days differential curing conditions.

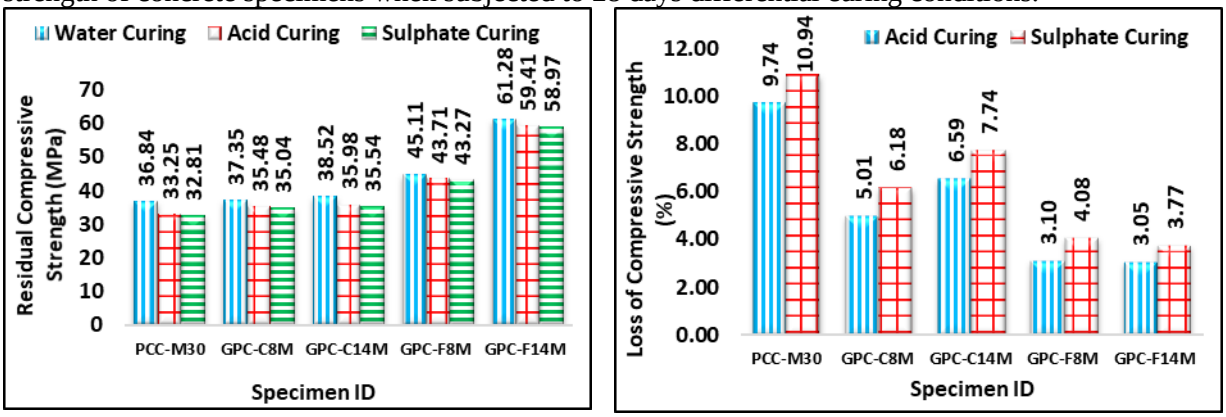

a. Residual Compressive Strength **b. Loss of Compressive Strength**

Fig. 6 Compressive Strength Variation of Concrete Specimens in Differential Curing Conditions

The low water absorption and low porosity of GPC contributed to the mix's increased compressive strength. While heat curing at 60oC for 24 hours made the product more porous, it also weakened its compressive strength due to the evaporation of moisture/water from the pores. When steel slag was used as a coarse aggregate in the geopolymer mix, it resulted in higher compressive strengths than conventional cement concrete. Local steel slag aggregate was less absorbent than crushed stone as coarse

aggregate material because of its low water absorption. Steel slag aggregate GPC, on the other hand, had a slightly higher reduction in strength because the aggregates were more porous than conventional aggregate, which resulted in a more active change.

4.2 Thermal Conditions

4.2.1 Density

Table 8 shows the test results pertaining to residual weight and percentage loss of weight of concrete specimens when subjected to elevated temperatures.

Table 8. Reduction and Loss in Density of Concrete Specimens at Elevated Temperatures

Specimen ID	Initial Weight of 28 days Specimen	Residual Weight @ 6 hrs of Heating (kg)			Loss of Weight @ 6 hrs of Heating (%)		
	kg	200ºC	400 ºC	600 ºC	200 ºC	400 ºC	600 ºC
PCC-M30	8.02	2.371	2.253	2.154	70.44	71.91	73.14
GPC-C8M	8.09	2.208	2.160	2.098	72.71	73.30	74.07
GPC-C14M	8.19	2.226	2.197	2.162	72.82	73.17	73.60
GPC-F8M	8.18	2.218	2.177	2.143	72.89	73.39	73.80
GPC-F14M	8.12	2.238	2.214	2.178	72.44	72.73	73.18

The Figure 7 shows the variations in the residual weight and percentage loss of weight of concrete specimens when subjected to elevated temperatures.

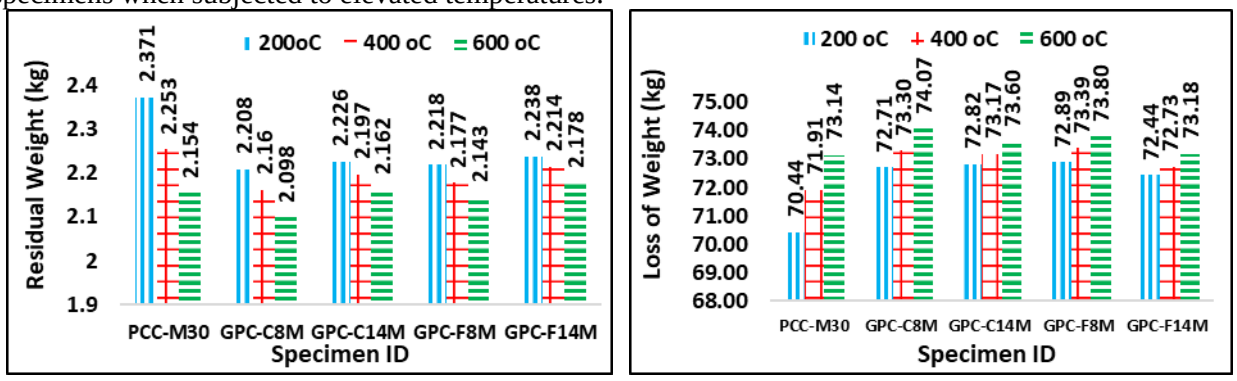

a. Residual Weight **b. Loss of Weight**

Fig.7 Density Variation of Concrete Specimens at Elevated Temperatures

From the results (Table 8 and Figure 7) it was observed that when the temperature increased, the percentage loss of weight of the PCC and GPC specimens also increased.

4.2.2 Compressive Strength

Table 9 shows the test results pertaining to residual the concrete's compressive strength and the percentage loss in that strength specimens when subjected to elevated temperatures.

Table 9. Reduction and Loss in Compressive Strength of Concrete Specimens at Elevated Temperatures

Specimen ID	28 days Compressive Strength	Residual Compressive Strength @ 6 hrs of Heating (MPa)			Loss of Compressive Strength @ 6 hrs of Heating (%)		
	MPa	200ºC	400 ºC	600 ºC	200 ºC	400 ºC	600 ºC
PCC-M30	36.84	29.94	23.04	16.14	18.73	37.46	56.19
GPC-C8M	37.35	32.30	30.78	24.53	13.52	17.59	34.32
GPC-C14M	38.52	33.47	31.95	25.70	13.11	17.06	33.28
GPC-F8M	45.11	40.06	38.54	32.29	11.19	14.56	28.42
GPC-F14M	61.28	56.23	54.71	48.46	8.24	10.72	20.92

The Figure 8 shows the variations in the residual compressive strength and percentage loss of compressive strength of concrete specimens when subjected to elevated temperatures.

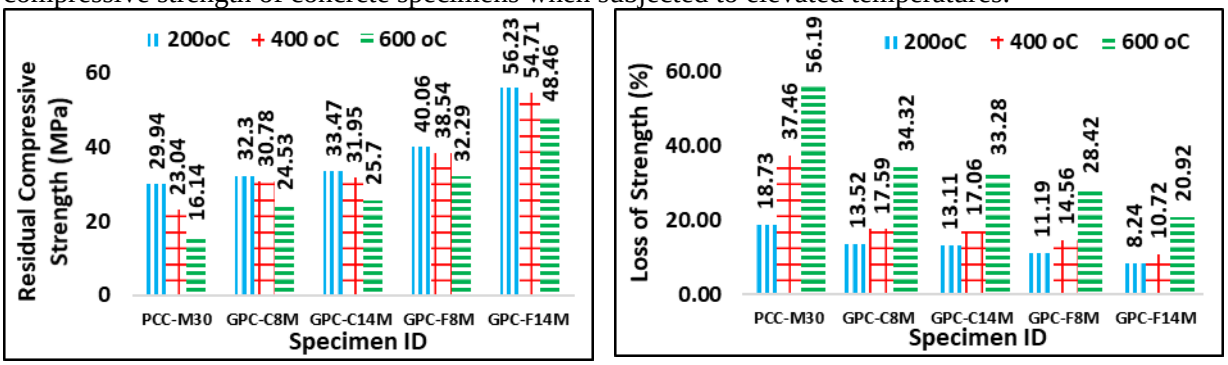

a. Residual Compressive Strength **b. Loss of Compressive Strength**

Fig. 8 Compressive Strength Variation of Concrete Specimens at Elevated Temperatures

From the results (Table 9 and Figure 8While ordinary cement concrete's residual compressive strength decreased as the temperature rose, Geopolymer concrete's compressive strength increased up to 6,000 degrees Celsius. Hence, it can be concluded that GPC possessed significant residual compressive strength than conventional PCC specimens.

4.2.3 Thermal Insulation

Figure 9 displays the surface contour as a representation for thermal insulation capacity of concrete specimens when subjected to peak sunny daytime temperature recorded at every one-hour interval between 9am to 6pm.

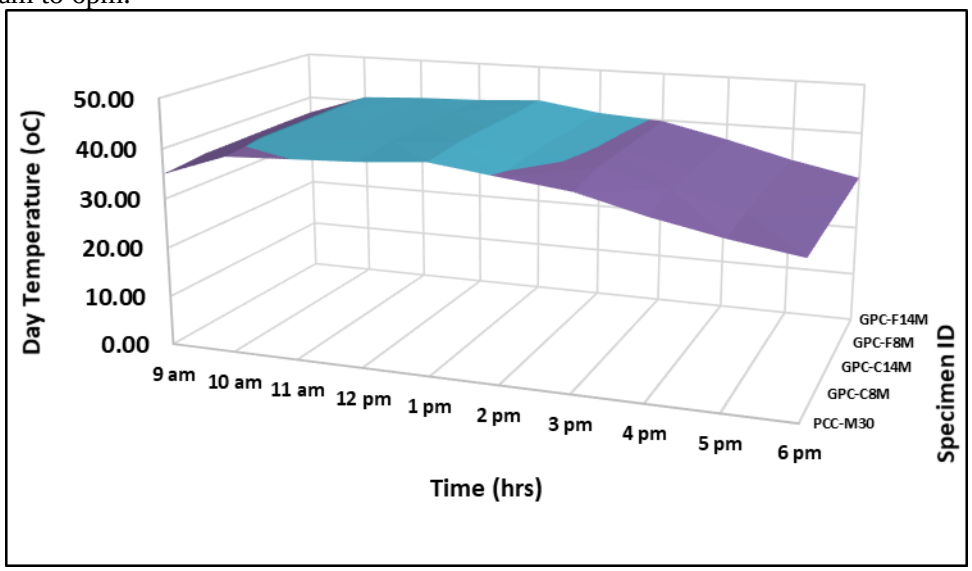

Fig. 9 Surface Contour of Thermal Insulation Capacity of Concrete Specimens Exposed to Daylight Temperature

From Figure.9, the variation in the thermal insulating capacity of the GPC specimens and PCC specimens was well defined. It was observed that both type of concrete specimens produced typical values exhibiting a similar behaviour under normal conditions. Hence, GPC specimens made of flyash as binder material, M-sand as fine aggregate and steel slag as coarse aggregate was found to be identical with conventional PCC specimens. No disparity was found between each other in thermal insulation characteristics.

4.2.4 Heat Dissipation

Figure 10 depicts the contour pattern of temperature gradient of concrete specimens due to dissipation of heat within a time period of 15 minutes.

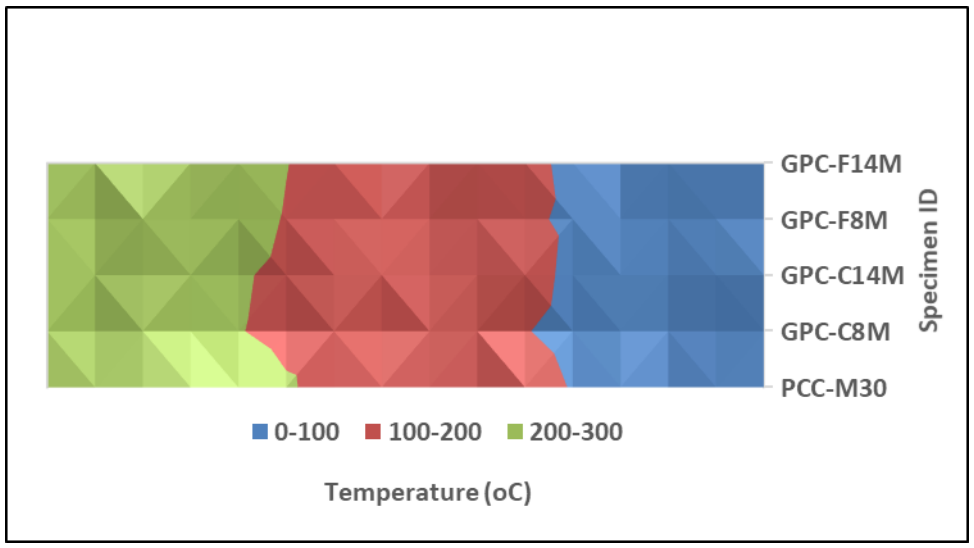

Fig. 10 Contour Showing Temperature Gradient of Concrete Specimens due to Dissipation of Heat

From Figure 10, the difference in the heat dissipating capacity between the PCC and GPC specimens was clearly identified. The results revealed that the GPC specimens released the heat inside the matrix at a faster rate than PCC specimens and hence it can be concluded that GPC specimen inherited more heat dissipating capacity than PCC specimens.

4.3 Microscopic Analysis

4.3.1. XRD Analysis

Images depicting geopolymer mixtures with distinct water-to-fly ash ratios are shown in Figure 11. Analyzing the samples, it was found that a large portion of the structure was still amorphous, and that the crystal gels formed around these samples had a broad band instead than sharp peaks at 30 degrees of 2theta. Additionally, quartz peaks from raw material that had not been reacted were found. In the literature on alkali-activated flyash geopolymer, so several statistics on the growth of various types of hydrate assemblages were discussed. The studies revealed that in class-C high calcium flyash-based geopolymer, the governing reactions were highly complex due to the presence of soluble Ca ions. Hydrate assemblages in the activated high calcium flyash differed from those in the activated low calcium flyash, highlighting the importance of calcium. The most important factor in class-C high calcium flyash was the location of the glass diffraction maximum, which formed the highest point in broadband X-ray patterns. That's not all: The dissolved calcium and silicate ions form C-S-H gels by reacting with CaOH2 precipitated from oxides and silicates and by replacing cations in the geopolymer.

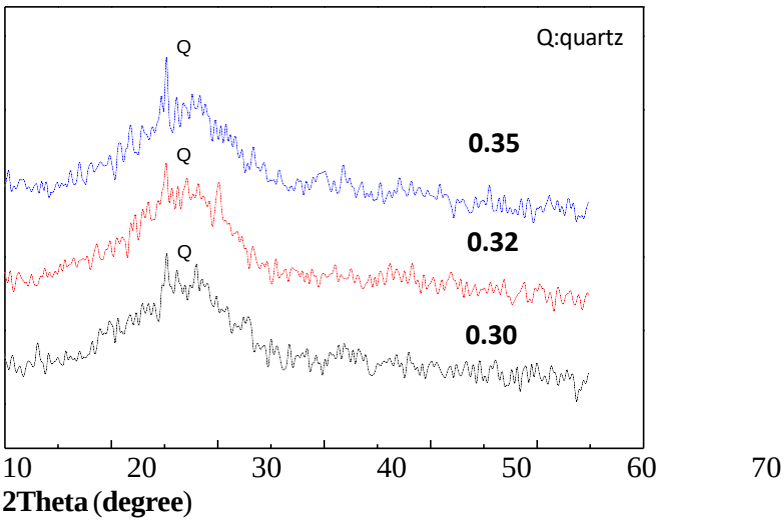

Fig. 11 XRD Image of Geopolymer Mix with different Water-to-Flyash Ratios.

4.3.2. SEM Analysis

Figure 12 shows the SEM micrographs of geopolymer mixes with varying water-to-fly ash ratios. The SEM pattern revealed that the geopolymer mix contained a relatively dense reacted product irrespective of the water-to-flyash ratios. This densely compacted structure of the mix as a result of reacted product was the reason to produce higher compressive strengths. The formation of cracks may be due to process involved during the compressive strength test.

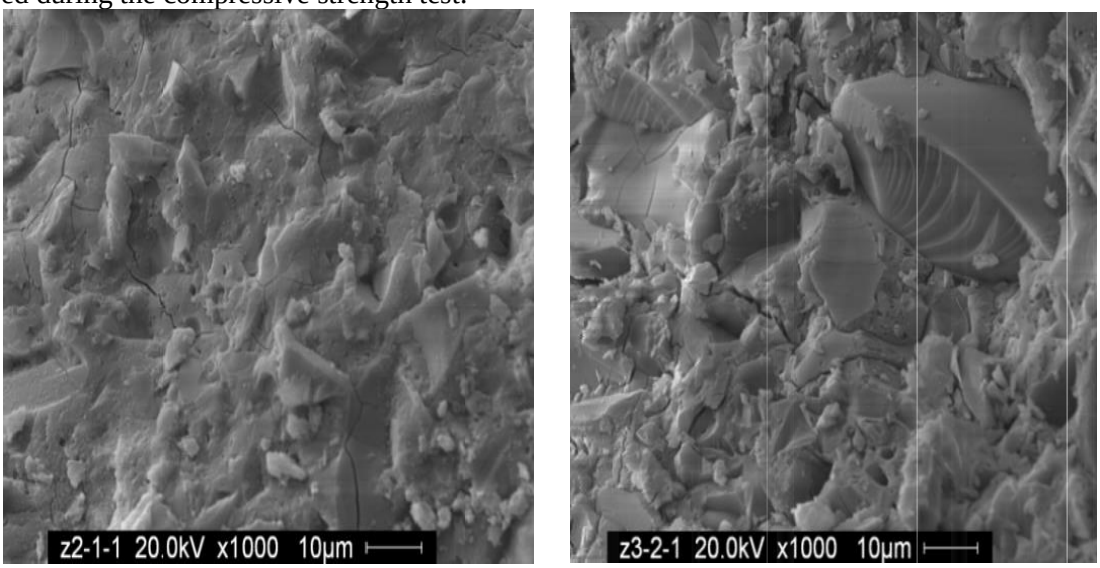

(**a**) W/F=0.32 (**b**) W/F=0.35

Fig. 12 SEM Images of Geopolymer Mix with different Water-to-Flyash Ratios

5 Conclusions

From the laborious experimental tests and results, the effect of class of flyash, molar concentration of NaOH and age of curing period on the durability properties of the geopolymer concrete subjected to microstructural analyses were examined and the following conclusions are drawn from its inferences:

- The residual weight of GPC specimens was high when compared to PCC specimen and hence the percentage loss of weight of GPC specimens was low when compared to PCC specimen under differential curing conditions.
- The 28 days residual compressive strength of GPC specimens was high when compared to PCC specimen and hence the percentage loss of compressive strength of GPC specimens was low when compared to PCC specimen under differential curing conditions.
- The residual weight of GPC specimens was high when compared to PCC specimen and hence the percentage loss of weight of GPC specimens was low when compared to PCC specimen at elevated temperatures.
- The 28 days residual compressive strength of GPC specimens was high when compared to PCC specimen and hence the percentage loss of compressive strength of GPC specimens was low when compared to PCC specimen at elevated temperatures.
- The XRD study of the microstructure analysis revealed that the geopolymer mix exhibited a broadband diffraction instead of a sharp diffraction pattern in 2θ condition.
- The SEM image of the microstructure analysis revealed that the geopolymer concrete mix exhibited a relatively dense compacted structure that resulted in low porosity, low water absorption and higher compressive strengths compared to conventional concrete mixes.
- In overall, GPC incorporating industrial waste by-products possessed excellent durability and microstructural properties and found to be an effective alternative concrete replacing the conventional concrete, which involves resource materials that depletes both nature and environment.

References

1. Xueying Li , Xinwei Ma , Shoujie Zhang and Enzu Zheng, Mechanical Properties and Microstructure of Class C Fly Ash-Based Geopolymer Paste and Mortar, *Materials* 2013, *6*, pp 1485-1495.

2. K.Arul priya, Strength and Durability Studies of M-Sand and Fly Ash Based Geopolymer Concrete, *International Journal of Trend in Research and Development*, Volume 3(3), May - Jun 2016, pp 90-97.

3. Chithambar Ganesh. A, Comparative Study on the Behaviour of Geopolymer Concrete using M-Sand and Conventional Concrete Exposed to Elevated Temperature, *International Journal of Civil Engineering and Technology (IJCIET)*, Volume 9, Issue 11, November 2018, pp. 981–989.

4. T. Srinivas and P. Geethanjali Rathod, Studies on the Behaviour of Geopolymer Concrete with Manufactured Sand as Fine Aggregate when Exposed to Elevated Temperatures, *International Journal of Research in Advent Technology (IJRAT) Special Issue "*ICADMMES 2018*",* pp 172-176.

5. O. M. Omar, A. M. Heniegal, G. D. Abd Elhameed, H. A. Mohamadien, Effect of Local Steel Slag as a Coarse Aggregate on Properties of Fly Ash Based-Geopolymer Concrete, *International Journal of Civil, Environmental, Structural, Construction and Architectural Engineering*, Vol:9, No:11, 2015, pp 1452-1460.

6. Suganya. N, Thirugnanasambandam. S, Experimental Investigation on Low Calcium Fly Ash Based Geopolymer Concrete using Steel Slag as Coarse Aggregate, *Journal of Emerging Technologies and Innovative Research (JETIR)*, February 2019, Volume 6, Issue 2, 2019, pp 364-369.

7. Rosicky Methode Kalombe, Victor Tunde Ojumu, Chuks Paul Eze, Sammy Mwasaha Nyale, John Kevern and Leslie Felicia Petrik, Fly Ash-Based Geopolymer Building Materials for Green and Sustainable Development, *Materials*, 2020, 13, 5699, pp 1-17.
8. Sarvenaz Moradikhou and Amir Bahador Moradikhou, Geopolymer Concrete Based on Class C Fly ash Cured at Ambient Condition, *Journal of Civil Engineering and Materials Application*, 2021 (December); 5(4), pp 177-195.
9. K.Mahendran and N.Arunachelam, Study on Utilization of Copper Slag as Fine Aggregate in Geopolymer Concrete, *International Journal of Applied Engineering Research*, Vol. 10 No.53, 2015, pp 336-340.
10. Ali I.M., Naje A.S, Al-Zubaidi H.A.M. and Al-Kateeb R.T., Performance Evaluation of Fly Ash-Based Geopolymer Concrete Incorporating Nano Slag, *Global NEST Journal*, Vol. 21, No 1, pp 70-75.
11. T. Srinivas and R. N. Koushik, Sulphate attack Resistance of Geo-polymer Concrete made with Partial Replacement of Coarse Aggregate by Recycled Coarse Aggregate, *International Journal of Innovative Technology and Exploring Engineering (IJITEE)*, Volume-8 Issue-12, October 2019, pp 112-117.
12. IS 383-1970: Specification for Coarse and Fine Aggregates from Natural Sources for Concrete, Bureau of Indian Standards, New Delhi, India.
13. IS 456-2000: Plain and Reinforced Concrete - Code of Practice, Bureau of Indian Standards, New Delhi, India.
14. IS 3812 (PART-1)-2003: Specification for Pulverized Fuel Ash, Part 1: For use as Pozzolana in Cement, Cement Mortar and Concrete, Bureau of Indian Standards, New Delhi, India.
15. IS 8112-2013: Specification for 43 Grade Ordinary Portland Cement, Bureau of Indian Standards, New Delhi, India.